Electronic Supporting Information

Discrete unusual mixed-bridged trinuclear $Co^{III}_2Co^{II}$ and pentanuclear Ni^{II} coordination complexes supported by phenolate-based ligand: theoretical and experimental magneto-structural study

Richa[a,#], Muni Rathnam[b,#], Akhilesh Kumar[c,g], Indresh Verma[c], Julia Kłak[*,d], Joan Cano[e], Antonio J. Mota[*,f], Amit Rajput[*,a] and Himanshu Arora[*,a]

[a]*School of Engineering and Sciences, G.D. Goenka University, Gurugram, India. E-mail: himanshuiitk2004@gmail.com,+91 8860185079.*

[b] *Department of Chemical Sciences, Indian Institute of Science Education and Research Kolkata, Mohanpur 741 246, India.*

[c] *Department of Chemistry, Indian Institute of Technology Kanpur, Kanpur 208 016, India*

[d] *Faculty of Chemistry, University of Wroclaw, Wroclaw 50-383, Poland.*

[e]*Department of Química Inorgànica/Instituto de Ciencia Molecular (ICMol), Facultat de Quimica de la Universitat de València, C/Catedrático Jose Beltrán 2, 46980 Paterna, València, Spain.*

[f]*Department of Inorganic Chemistry, Faculty of Science, University of Granada, 18071, Granada, Spain. E-mail: mota@ugr.es*

[g]*Department of Chemistry, Axis Institute of Technology & Management Kanpur, Kanpur, India*

[#]*Both the authors have equal contribution.*

1. UV-Vis of **1**-**2** in CH_3CN Fig. S1-S2

2. Field dependence of the magnetization (*M* per $Co^{III}_2Co^{II}$ entities) for **1** Fig. S3

3. Field dependence of the magnetization (M per Ni_5 entities) for **2** Fig. S4

4. Additional discussion of magnetic studies of complex **1**.

5. Calculated magnetization at different temperatures for Co3 in complex **1** Fig. S5

6. Orientation of D_{zz}, D_{xx} and D_{yy} for Co3 in complex **1** Fig. S6

7. View of the calculated complexes **1AF** (up, left), **1F** (up, right) and **1Fwa** (bottom), in order to reveal the influence of the AF and F moieties, and the acetate bridges on the global magnetic behavior of the complex. Fig. S7

8. Addition discussion of theoretical studies of complex **2**.

9. Selected bond lengths [Å] and angles [°] of **1** and **2** Table S1
10. Bond Valence Calculation Table of complex **1** Table S2
11. Calculated spin densities of the magnetic centers of complex **2** Table S3

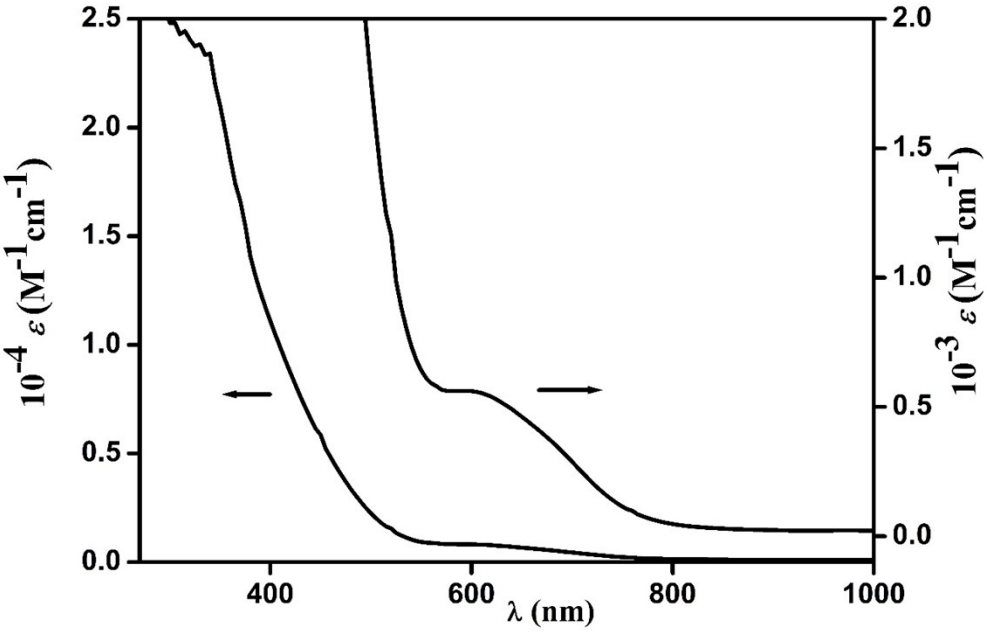

Fig. S1. Absorption spectra of $[Co^{II/III}_3(\mu\text{-}OL)_2(\mu\text{-}OOCCH_3)_2(\mu\text{-}N_3)_2(N_3)_2]$ **(1)** in CH_3CN.

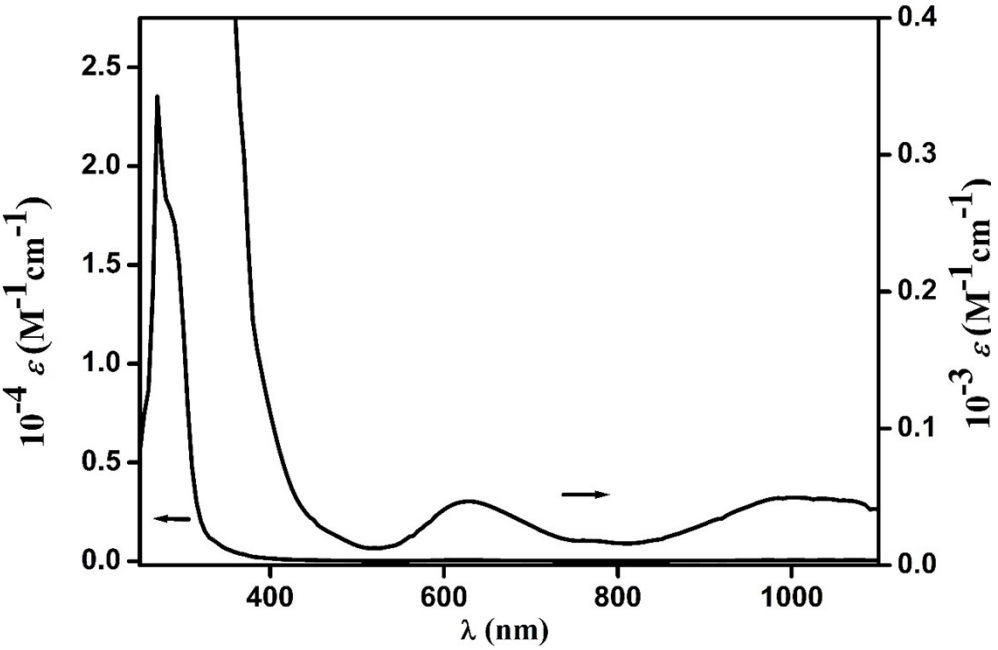

Fig. S2. Absorption spectra of $[Ni^{II}_5(\mu\text{-}OL)_4(\mu\text{-}OOCCH_3)_2(OOCCH_3)_2(\mu\text{-}N_3)_2]$ **(2)** in CH_3CN.

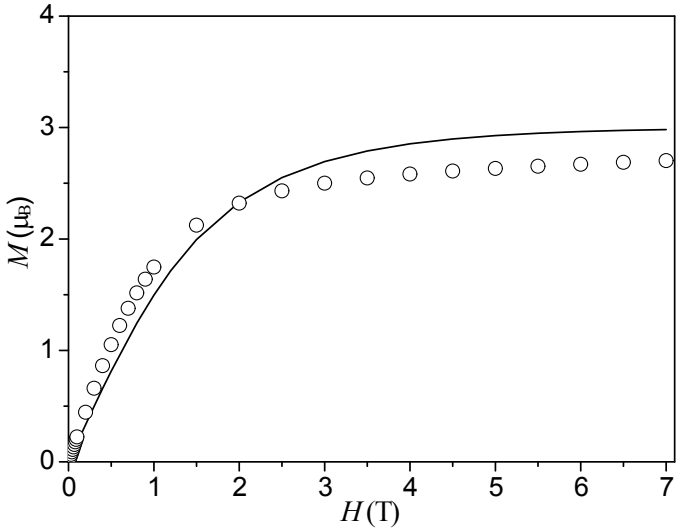

Fig. S3. Field dependence of the magnetization (M per $Co^{III}_2Co^{II}$ entities) for **1**. The solid line is the Brillouin function curve for the system of one uncoupled spin with $S = 3/2$ and $g = 2.0$ in the absence of zero-field splitting.

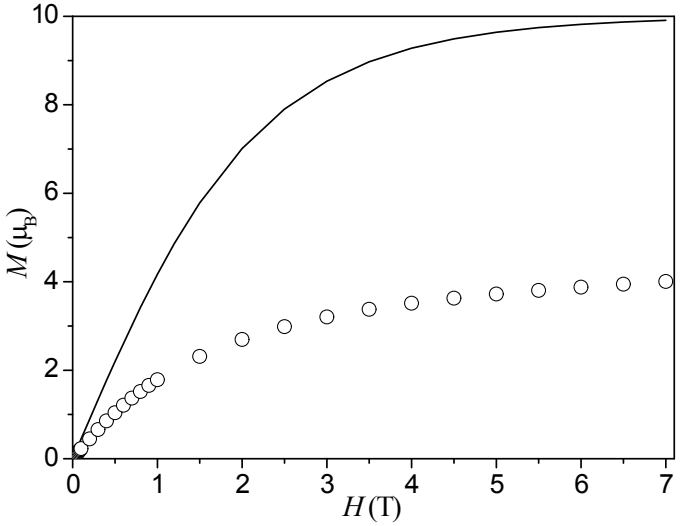

Fig. S4. Field dependence of the magnetization (M per Ni_5 entities) for **2**. The solid line is the Brillouin function curve for the system of five uncoupled spins with $S = 1$ and $g = 2.0$ in the absence of zero-field splitting.

Additional discussion of magnetic studies of complex **1**.The magnetic susceptibility for a magnetically isolated cobalt(II) derived through Hamiltonian is shown in eq (2-5):[4]

$$\chi_m = \frac{\chi_{//} + 2\chi_{\perp}}{3} \tag{2}$$

$$\chi_{II} = \frac{N\beta^2 g_{II}^2}{4kT} \cdot \frac{1 + 9\exp\left(-\frac{2D}{kT}\right)}{1 + \exp\left(-\frac{2D}{kT}\right)} \tag{3}$$

$$\chi_{\perp} = \frac{N\beta^2 g_{\perp}^2}{4kT} \cdot \frac{4 + 3\frac{kT}{D}\left[1 - \exp\left(-\frac{2D}{kT}\right)\right]}{1 + \exp\left(-\frac{2D}{kT}\right)} \tag{4}$$

Taking to account the possibility of presence of weak intermolecular magnetic exchange, the eq. 2 must be modified by including a molecular field correction term (zJ').[4] This yields the equation (eq.5):

$$\chi_m^{corr} = \frac{\chi_m}{1 - \frac{2zJ'}{N\beta^2 g^2} \cdot \chi_m} \tag{5}$$

In the fitting process, we have neglected the rhombic components of the zero-field splitting and considered $g_{\parallel} = g_{\perp} = g$ (average Landé factor) in order to avoid overparameterization.

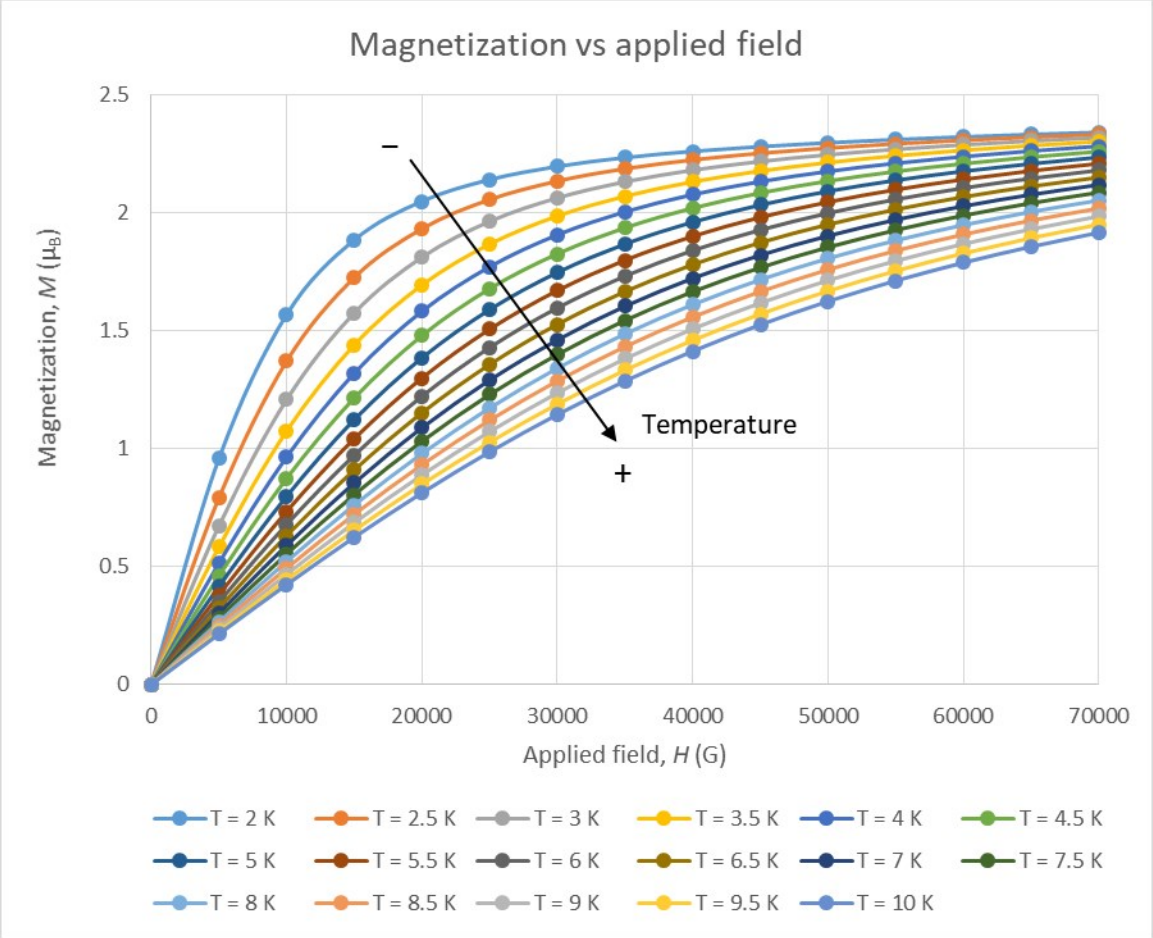

Fig. S5. Theoretical simulation of the magnetization in function of the applied field and the temperature for Co3 in complex **1**.

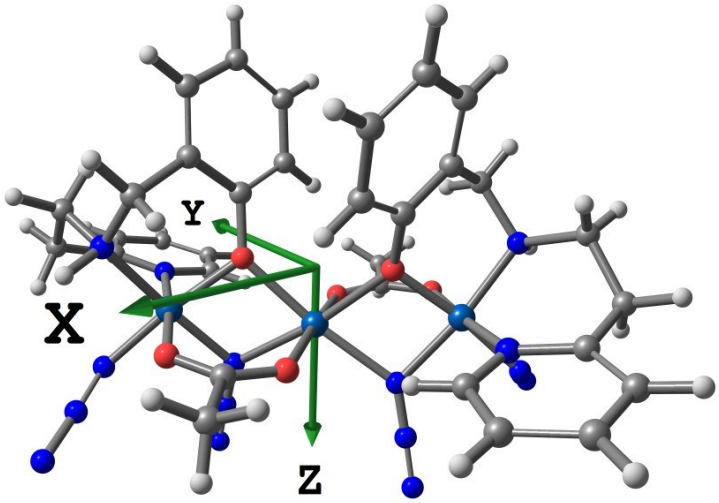

Fig. S6. Representation of the calculated orientation for the components D_{zz}, D_{xx} and D_{yy} (appearing as Z, X and Y, respectively) to the magnetic anisotropy for Co3 in complex **1**.

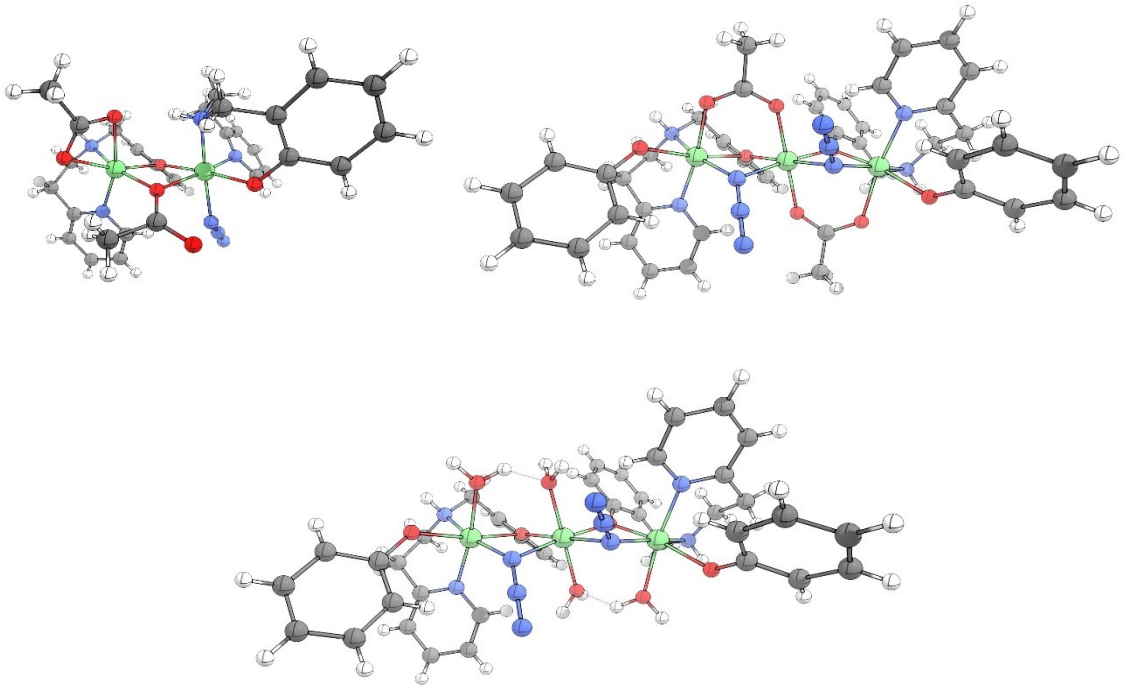

Fig. S7. View of the calculated complexes **1AF** (up, left), **1F** (up, right) and **1Fwa** (bottom), in order to reveal the influence of the AF and F moieties, and the acetate bridges on the global magnetic behavior of the complex.

One could expect that, besides the Ni-Ni bridges, the ferromagnetic part of the complex (Ni2-Ni3-Ni4 moieties) could modulate the coupling constant of the AF part (Ni1-Ni2 and Ni4-Ni5 moieties) and vice versa. In order to know the extent of this mutual effect, we have calculated the magnetic coupling constants for several new complexes: one, **1AF**, the AF part where only operates a unique magnetic pathway defined by J_1, formed by Ni1 and Ni2 centers by keeping all their ligands as found in the crystal structure, and other, **1F**, the ferromagnetic part where two magnetic pathways namely, J_2 and J_4 are operative, formed by Ni2, Ni3 and Ni4 centers keeping all their ligands as found in the crystal structure except the phenoxy moiety that we cut to strictly have a phenoxo ligand. See Fig. S7 and the related text in the SI for more information about the effect of these changes.For the former (**1AF**) we get a new J_1 magnetic coupling constant of −21.1 cm^{-1}, very similar to that of the title compound, see Table 4. For the later (**1F**) we get new values of the corresponding magnetic coupling constants of +25.8 and −0.6 cm^{-1}, respectively for J_2 and J_4. These values therefore demonstrate that both parts of the pentanuclear complex (the AF and F coupled) are almost independent from a magnetic point of view and that both behave as two independent complexes with little influence on each other.

Furthermore, in order to understand the importance of the *syn-syn* bridging acetato ligands in the magnetic behavior of the ferromagnetic part of the complex, we recalculate complex **1F** by replacing the acetate ligands by water molecules, **1Fwa** in Fig. S7, keeping the oxygen positions and adding the needed hydrogen atoms. This operation resulted in new magnetic coupling constants values of +19.5 and −4.3 cm^{-1}, respectively for J_2 and J_4 (to compare with +25.8 and −0.6 cm^{-1}, respectively), thus revealing the ferromagnetic contribution of the acetate bridge for both (J_2 and J_4) magnetic pathways.

Table S1. Selected bond lengths [Å] and angles [°] of $[Co^{III}_2Co^{II}(\mu\text{-}OL)_2(\mu\text{-}OOCCH_3)_2(\mu\text{-}N_3)_2(N_3)_2]\cdot Et_2O$ **(1)** and $[Ni^{II}_5(\mu\text{-}OL)_4(\mu\text{-}OOCCH_3)_2(OOCCH_3)_2(\mu\text{-}N_3)_2]\cdot CH_3CN$ **(2)**.

$[Co^{III}_2Co^{II}(\mu\text{-}OL)_2(\mu\text{-}OOCCH_3)_2(\mu\text{-}N_3)_2(N_3)_2]\cdot Et_2O$ **(1)**			
C1–O1	1.347(5)	C17–O4	1.354(5)
C15–O2	1.244(6)	C15–O3	1.260(6)
C31–O5	1.230(7)	C31–O6	1.277(6)
O1–Co1–O1#	180.00(16)	O2–Co1–O2#	180.0(1)
O2–Co1–O1	86.81(12)	O2–Co1–O1#	93.19(12)
O1–Co1–N3	74.33(13)	O1–Co1–N3#	105.67(13)
O2–Co1–N3	87.01(13)	O2–Co1–N3#	92.99(13)
N3–Co1–N3#	180.0(2)	O4–Co3–N11	73.15(15)
O4–Co3–O4$	98.88(16)	O4–Co3–O5	88.31(14)
O4–Co3–N11$	171.86(15)	O5–Co3–O5$	174.9(2)
O4–Co3–O5$	95.04(13)	O5–Co3–N11$	90.70(17)
O5–Co3–N11	86.53(16)	N11–Co3–N11$	114.9(3)
O1–Co2–O3	92.43(13)	O1–Co2–N1	90.74(14)
O1–Co2–N2	93.66(15)	O1–Co2–N3	81.82(15)
O1–Co2–N6	174.28(18)	O3–Co2–N1	175.95(17)
O3–Co2–N3	88.67(15)	O3–Co2–N2	83.77(16)
O3–Co2–N6	88.08(17)	N1–Co2–N2	93.52(17)
N1–Co2–N3	94.28(17)	N2–Co2–N3	171.03(17)
N1–Co2–N6	89.02(17)	N2–Co2–N6	92.1(2)
N3–Co2–N6	92.50(18)	N9–Co4–N10	92.64(18)
O4–Co4–O6	91.42(14)	O4–Co4–N9	91.60(15)
O4–Co4–N10	93.54(15)	O4–Co4–N11	81.30(16)
O4–Co4–N14	173.0(2)	O6–Co4–N9	175.33(18)
O6–Co4–N10	83.62(17)	O6–Co4–N11	90.73(17)
O6–Co4–N14	89.81(17)	N9–Co4–N11	93.25(18)
N10–Co4–N11	172.27(18)	N9–Co4–N14	87.63(18)

N10–Co4–N14	93.5(2)	N11–Co4–N14	91.8(3)
C1–O1–Co1	134.5(3)	C1–O1–Co2	123.9(3)
C17–O4–Co3	134.4(3)	C17–O4–Co4	122.8(3)
C15–O2–Co1	127.9(3)	C15–O3–Co2	130.0(3)
C31–O5–Co3	128.2(4)	C31–O6–Co4	127.6(4)
N4–N3–Co1	136.8(4)	N4–N3–Co2	124.7(4)
N7–N6–Co2	120.6(4)	N12–N11–Co3	135.3(5)
N12–N11–Co4	126.2(5)		
# [1–x, 1–y, 1–z], $ [1–x, y, 1.5–z]			

$[Ni^{II}_5(\mu\text{-}OL)_4(\mu\text{-}OOCCH_3)_2(OOCCH_3)_2(\mu\text{-}N_3)_2]\cdot CH_3CN$ **(2)**			
C1–O1	1.329(3)	C15–O4	1.345(3)
C29–O2	1.249(3)	C29–O3	1.284(3)
C31–O5	1.268(3)	C31–O6	1.265(3)
O1–Ni1–O1#	105.00(9)	O1–Ni1–O2	87.70(6)
O1–Ni1–N3	172.97(7)	O1–Ni1–O2#	94.47(6)
O1–Ni1–N3#	81.44(7)	O2–Ni1–N3#	88.56(7)
O2–Ni1–O2#	176.43(9)	O2–Ni1–N3	88.97(7)
N3–Ni1–N3#	92.29(10)	N2–Ni2–N3#	169.30(7)
O1–Ni2–O3	93.72(6)	O1–Ni2–O4	169.66(6)
O3–Ni2–O4	75.96(6)	O1–Ni2–N1	95.58(7)
O1–Ni2–N2	90.18(7)	O1–Ni2–N3	80.75(7)
O4–Ni2–N1	94.73(7)	O4–Ni2–N2	90.60(7)
O4–Ni2–N3#	97.31(7)	N1–Ni2–O3	170.64(7)
N2–Ni2–O3	90.59(7)	N3–Ni2–O3#	84.39(7)
N1–Ni2–N2	90.46(7)	N1–Ni2–N3#	96.04(7)
N4–N3–Ni1	116.13(15)	O3–Ni3–O4	78.19(6)
O3–Ni3–O5	88.82(6)	O4–Ni3–O5	99.39(6)
O4–Ni3–O6	160.42(7)	O3–Ni3–O6	95.93(6)

O5–Ni3–O6	61.56(6)	O3–Ni3–N6	97.15(7)
O3–Ni3–N7	167.83(7)	O4–Ni3–N6	96.43(7)
O4–Ni3–N7	92.42(7)	O5–Ni3–N6	163.94(7)
O5–Ni3–N7	85.06(7)	O6–Ni3–N6	102.85(7)
O6–Ni3–N7	90.40(7)	N6–Ni3–N7	91.54(8)
N4–N3–Ni2#	134.19(16)	Ni1–O1–C1	135.02(14)
Ni2–O1–C1	123.76(13)	Ni2–O4–C15	132.91(14)
Ni3–O4–C15	120.76(14)	Ni2–O3–C29	125.68(15)
Ni3–O3–C29	131.37(15)	Ni1–O2–C29	130.58(15)
Ni3–O5–C31	87.87(14)	Ni3–O6–C31	90.65(15)
# [1.5–x, y, 1–z]			

Table S2. Bond Valence Calculation of **1**

	Trans Conformation			
	R	R0	(R0-R)/B	Sij = exp{(R0-R)/B}
Co1–O1	2.054(3)	1.685	-0.997	0.37
Co1–N3	2.137(5)	1.72	-1.127	0.32
Co1–O2	2.049(4)	1.685	-0.983	0.37
Co1–O1	2.054(3)	1.685	-0.997	0.37
Co1–N3	2.137(5)	1.72	-1.127	0.32
Co1–O2	2.049(4)	1.685	-0.983	0.37
			V	2.12
Co2–O1	1.914(4)	1.637	-0.749	0.47
Co2–N1	1.953(5)	1.69	-0.711	0.49
Co2–N2	1.961(5)	1.69	-0.732	0.48
Co2–O3	1.911(3)	1.637	-0.740	0.48
Co2–N3	1.953(5)	1.69	-0.711	0.49
Co2–N6	1.928(5)	1.69	-0.643	0.53
			V	2.94
	Cis Conformation			
Co3–O4	2.058(4)	1.685	-1.01	0.36
Co3–N11	2.137(5)	1.72	-1.127	0.32

Co3–O5	2.035(4)	1.685	-0.946	0.39
Co3–O4	2.058(4)	1.685	-1.01	0.36
Co3–N11	2.137(5)	1.72	-1.127	0.32
Co3–O5	2.035(4)	1.685	-0.946	0.39
			V	2.14
Co4–O4	1.902(3)	1.637	-0.716	0.49
Co4–N9	1.965(4)	1.69	-0.743	0.47
Co4–N11	1.937(5)	1.69	-0.667	0.51
Co4–O6	1.945(3)	1.637	-0.832	0.43
Co4–N10	1.961(5)	1.69	-0.732	0.48
Co4–N14	1.914(5)	1.69	-0.605	0.55
			V	2.93

Table S3. Calculated spin densities of the magnetic centers (as shown in Table 4) for all the calculated states. Darker backgrounds in cells represent the spin down centers in each case.

State (Multiplicity)	Ni1	Ni2	Ni3	Ni4	Ni5
11	+1.6637	+1.6570	+1.6690	+1.6570	+1.6637
7[a]	−1.6601	+1.6554	+1.6691	+1.6569	+1.6637
7b	+1.6595	−1.6588	+1.6732	+1.6569	+1.6637
7c	+1.6643	+1.6605	−1.6778	+1.6605	+1.6643
3[a]	−1.6643	−1.6604	+1.6734	+1.6569	+1.6637
3b	−1.6595	+1.6589	−1.6776	+1.6605	+1.6643
3c	−1.6601	+1.6554	+1.6734	−1.6588	+1.6595
3d	−1.6601	+1.6554	+1.6693	+1.6554	−1.6601
3e	+1.6601	−1.6553	−1.6736	+1.6604	+1.6643
3f	+1.6595	−1.6589	+1.6775	−1.6589	+1.6595